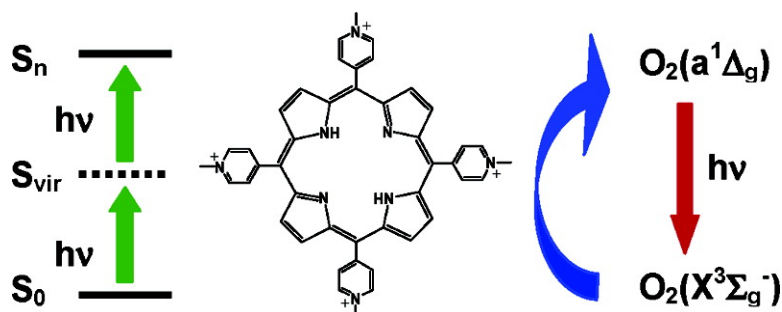


Two-Photon Photosensitized Production of Singlet Oxygen in Water

Peter K. Frederiksen, Sean P. McIlroy, Christian B. Nielsen, Lars Nikolajsen, Esben Skovsen, Mikkel Jrgensen, Kurt V. Mikkelsen, and Peter R. Ogilby

J. Am. Chem. Soc., **2005**, 127 (1), 255-269 • DOI: 10.1021/ja0452020 • Publication Date (Web): 10 December 2004

Downloaded from <http://pubs.acs.org> on March 24, 2009



More About This Article

Additional resources and features associated with this article are available within the HTML version:

- Supporting Information
- Links to the 23 articles that cite this article, as of the time of this article download
- Access to high resolution figures
- Links to articles and content related to this article
- Copyright permission to reproduce figures and/or text from this article

[View the Full Text HTML](#)

Two-Photon Photosensitized Production of Singlet Oxygen in Water

Peter K. Frederiksen,[†] Sean P. McIlroy,[†] Christian B. Nielsen,^{†,§} Lars Nikolajsen,[‡] Esben Skovsen,[†] Mikkel Jørgensen,[§] Kurt V. Mikkelsen,[‡] and Peter R. Ogilby^{*,†}

Contribution from the Department of Chemistry, University of Aarhus, DK-8000 Århus, Denmark; Department of Chemistry, University of Copenhagen, DK-2100 Copenhagen, Denmark; and Polymer Department, Risø National Laboratory, DK-4000 Roskilde, Denmark

Received August 9, 2004; E-mail: progilby@chem.au.dk

Abstract: Singlet molecular oxygen ($a^1\Delta_g$) has been produced and optically detected in time-resolved experiments upon nonlinear two-photon excitation of a photosensitizer dissolved in water. For a given sensitizer, specific functional groups that impart water solubility and that give rise to larger two-photon absorption cross sections are, in many cases, not conducive to the production of singlet oxygen in high yield. This issue involves the competing influence of intramolecular charge transfer that can be pronounced in aqueous systems; more charge transfer in the chromophore facilitates two-photon absorption but decreases the singlet oxygen yield. This phenomenon is examined in a series of porphyrins and vinyl benzenes.

Introduction

The lowest excited electronic state of molecular oxygen, singlet molecular oxygen ($a^1\Delta_g$), is an intermediate in many oxidation reactions.^{1,2} In systems of importance to biology and medicine, these reactions often occur in heterogeneous, water-containing, phase-separated samples.^{3,4} Thus, for work in such systems, it could be of great use to both produce and detect singlet oxygen in time- and space-resolved experiments.

Singlet oxygen can be readily and efficiently produced upon irradiation of a sensitizer which, in turn, transfers its energy of excitation to ground-state oxygen ($X^3\Sigma_g^-$).⁵ Sensitizers can be a chromophore inherent to a given system, as is the case with many functional polymers.⁶ Alternatively, a sensitizer can be specifically added to a system, as in the case of photodynamic therapy where light is used as a medical tool to selectively kill cells.⁴

Over the past four decades in which the photosensitized production of singlet oxygen has been extensively studied, sensitizer excitation has always been achieved via a linear one-photon transition between the sensitizer ground state, S_0 , and a singlet excited state of the sensitizer, S_n .⁵ After excitation, singlet oxygen is, in general, produced most efficiently upon oxygen

quenching of the sensitizer triplet state, T_1 , formed upon intersystem crossing, $S_1 \rightarrow T_1$.⁵

It has recently been demonstrated that singlet oxygen can also be produced upon nonlinear two-photon excitation of a sensitizer.^{7–9} In this case, an excited-state S_m is populated as a consequence of the less-probable simultaneous absorption of two lower energy photons. The transition proceeds via a virtual state, $S_0 \rightarrow S_{vir} \rightarrow S_m$, and follows selection rules that can differ from those for a one-photon transition. Note that, in this scheme, irradiation at a wavelength that does not coincide with the more dominant one-photon transition facilitates depth penetration in samples that might otherwise be opaque. Most importantly, however, is the opportunity to selectively populate an excited state at the point of a focused laser beam where a spatial domain of sufficiently high fluence can be obtained. In short, two-photon excitation of a sensitizer with a focused laser imparts spatial resolution to a singlet oxygen experiment.

Over the past ~25 years, a variety of techniques have been developed to detect singlet oxygen in time-resolved optical spectroscopic experiments.⁵ In the course of this work, it was established that the medium in which oxygen is dissolved significantly influences the experiment performed. In H_2O , where the singlet oxygen lifetime is comparatively short, ~3.5 μs ,^{10,11} and the rate constants for radiative transitions are small,^{12–14} optical detection of singlet oxygen can provide

[†] University of Aarhus.

[‡] University of Copenhagen.

[§] Risø National Laboratory.

(1) Foote, C. S. *Acc. Chem. Res.* **1968**, *1*, 104–110.

(2) Frimer, A. A., Ed. *Singlet Oxygen*; CRC Press: Boca Raton, FL, 1985; Vol. I–IV.

(3) Oleinick, N. L.; Morris, R. L.; Belichenko, I. *Photochem. Photobiol. Sci.* **2002**, *1*, 1–21.

(4) Dougherty, T. J.; Gomer, C. J.; Henderson, B. W.; Jori, G.; Kessel, D.; Korbelik, M.; Moan, J.; Peng, Q. *J. Natl. Cancer Inst.* **1998**, *90*, 889–905.

(5) Schweitzer, C.; Schmidt, R. *Chem. Rev.* **2003**, *103*, 1685–1757.

(6) Dam, N.; Scurlock, R. D.; Wang, B.; Ma, L.; Sundahl, M.; Ogilby, P. R. *Chem. Mater.* **1999**, *11*, 1302–1305.

(7) Frederiksen, P. K.; Jørgensen, M.; Ogilby, P. R. *J. Am. Chem. Soc.* **2001**, *123*, 1215–1221.

(8) Poulsen, T. D.; Frederiksen, P. K.; Jørgensen, M.; Mikkelsen, K. V.; Ogilby, P. R. *J. Phys. Chem. A* **2001**, *105*, 11488–11495.

(9) Karotki, A.; Drobizhev, M.; Kruk, M.; Spangler, C.; Nickel, E.; Mamar-dashvili, N.; Rebane, A. *J. Opt. Soc. Am. B.* **2003**, *20*, 321–332.

(10) Rodgers, M. A. J.; Snowden, P. T. *J. Am. Chem. Soc.* **1982**, *104*, 5541–5543.

(11) Egorov, S. Y.; Kamalov, V. F.; Koroteev, N. I.; Krasnovsky, A. A.; Toleutau, B. N.; Zinukov, S. V. *Chem. Phys. Lett.* **1989**, *163*, 421–424.

unique challenges. In biologically significant aqueous environments, the difficulties of detecting singlet oxygen can be further exacerbated due to the presence of quenchers that can reduce the singlet oxygen lifetime into the nanosecond domain.^{15,16}

In earlier work, we established that, in solutions of toluene, singlet oxygen could be produced upon two-photon irradiation of a sensitizer and optically detected in a time-resolved experiment via its $a^1\Delta_g - X^3\Sigma_g^-$ phosphorescence.^{7,8} In the present study, we set out to examine issues pertinent to the creation and detection of singlet oxygen in time-resolved, two-photon photosensitized experiments performed in water. We were particularly interested in examining the potentially unique aspects important to the design and development of viable, water-soluble two-photon singlet oxygen sensitizers. Although much has been published on the design of hydrophobic molecules with a large probability for two-photon absorption (i.e., the so-called two-photon absorption cross section),^{17–19} the application of this information to the development of an efficient water-soluble singlet oxygen sensitizer is not a trivial exercise. Moreover, because the quantum efficiency of singlet oxygen phosphorescence in water is ~ 100 times smaller than that in toluene,¹² we wanted to ascertain if it was possible to detect singlet oxygen in a time-resolved emission experiment upon two-photon excitation of a sensitizer. In turn, this would allow us to assess whether it is realistic to even consider the application of two-photon imaging techniques²⁰ to the study of singlet oxygen in heterogeneous aqueous systems.

Experimental Section

Apparatus and Techniques. Our earlier two-photon experiments were performed using nanosecond lasers.^{7,8} As our experiments have evolved, we have increasingly relied on femtosecond lasers that have spatial and temporal profiles that are more conducive to these nonlinear studies. Indeed, because results obtained from such nonlinear experiments depend significantly on the characteristics of the excitation source,^{21–23} a reasonable amount of instrumental detail should be provided to support our results.

A. Sample Irradiation. The heart of our system is a Ti:sapphire laser (Spectra Physics, Tsunami 3941) pumped by a Spectra Physics Millennia Vs Nd:YAG laser. The Tsunami operates at an 80 MHz repetition rate and can be tuned over the range ~ 725 – 910 nm. The temporal pulse width, ~ 75 – 95 fs (fwhm), is wavelength dependent and has a Gaussian profile (see Supporting Information, Appendix 1).

The output of the Tsunami can be amplified (Spectra Physics Spitfire pumped by a Spectra Physics Evolution Nd:YLF laser). Although the

process of amplification reduces the range of accessible wavelengths to ~ 765 – 845 nm and slightly increases the pulse width to ~ 100 – 120 fs (fwhm), it has the desirable feature of reducing the pulse repetition rate to 1 kHz. This is important for the time-resolved detection of singlet oxygen whose lifetime, τ_Δ , in most solvents of interest is in the microsecond domain [i.e., $\tau_\Delta < (1 \text{ kHz})^{-1}$].

The intensity of the laser beam incident on the sample was adjusted by rotating the polarization of the beam with a half-wave plate (Thorlabs model WPH05M-830) and then passing the resultant beam through a fixed polarized optic (Thorlabs model GT-10B Glan-Taylor Polarizer). Laser powers were then measured at this point using an Ophir Nova digital meter with a NIST-traceable, calibrated detection head with a specified accuracy of 1%. Thereafter, calibrated neutral density filters were added to further reduce the intensity of the beam. Finally, we accounted for the transmittance of the front window of the sample cuvette, thus giving an accurate measure of the power actually incident on the sample.

A 1 cm path length sample cuvette was mounted in a light-tight housing with a small entrance hole for the laser beam. Unless otherwise noted, the sample was irradiated using beams that had a Gaussian radial profile with a waist of either $300 \pm 20 \mu\text{m}$ or $600 \pm 20 \mu\text{m}$ (see Supporting Information, Appendix 2).

B. Signal Collection and Processing. Luminescence from the sample was collected and collimated using a 2.5 cm focal length lens. The collection efficiency was enhanced by placing a parabolic mirror on the backside of the cuvette. The light detected was spectrally isolated with interference filters and was focused with a second lens onto the active area of a photomultiplier tube, PMT (Hamamatsu model R5509-42, operated at -80°C , rise time of 3 ns).

The output of the PMT was amplified (Stanford Research Systems model 445 preamplifier) and sent to a photon counter (Stanford Research Systems model 400). When recording time-resolved data, the width of the photon-counter sampling window was reduced to a value that was small compared to the overall temporal profile of the signal, and counts were accumulated as this window was successively moved across the signal using a delayed trigger.

C. Relative Measurements of the Two-Photon Absorption Cross Section. For a given sensitizer, values of the two-photon absorption cross section were determined relative to those of 2,5-dicyano-1,4-bis-(2-(4-diphenylaminophenyl)viny)benzene, **CNPhVB** (see structure in Table 1). This latter molecule was chosen as a standard because its two-photon behavior has been studied by a number of investigators^{24,25} and, in addition to being strongly fluorescent, it produces a modest amount of singlet oxygen via sensitization (in toluene, **CNPhVB** has a singlet oxygen quantum yield, ϕ_Δ , of 0.13 ± 0.02 determined against the standard perinaphthenone with $\phi_\Delta = 1.0^{26}$).

In an independent experiment, we recorded the fluorescence excitation spectrum of **CNPhVB** upon two-photon irradiation of **CNPhVB**. The fluorescence signals monitored were corrected for wavelength-dependent changes in the spatial and temporal profiles of the laser pulse at the sample (a beam with a Gaussian waist of $\sim 110 \mu\text{m}$ was used for these experiments).^{9,21,27} The results obtained yielded the two-photon absorption profile of **CNPhVB** (Figure 4, vide infra).

Upon irradiation at a specific wavelength, relative values for the two-photon absorption cross section of a given molecule were obtained by comparing the singlet oxygen phosphorescence intensity recorded upon two-photon excitation of that molecule to the singlet oxygen phosphorescence intensity recorded upon two-photon excitation of **CNPhVB**.^{7,8} In this experiment, we assume that the yield of singlet oxygen produced upon two-photon excitation is the same as that

- (12) Scurlock, R. D.; Nonell, S.; Braslavsky, S. E.; Ogilby, P. R. *J. Phys. Chem.* **1995**, *99*, 3521–3526.
- (13) Poulsen, T. D.; Ogilby, P. R.; Mikkelsen, K. V. *J. Phys. Chem. A* **1998**, *102*, 9829–9832.
- (14) Andersen, L. K.; Ogilby, P. R. *J. Phys. Chem. A* **2002**, *106*, 11064–11069.
- (15) Kanofsky, J. R. *Photochem. Photobiol.* **1991**, *53*, 93–99.
- (16) Niedre, M.; Patterson, M. S.; Wilson, B. C. *Photochem. Photobiol.* **2002**, *75*, 382–391.
- (17) Albota, M.; Beljonne, D.; Brédas, J.-L.; Ehrlich, J. E.; Fu, J.-Y.; Heikal, A. A.; Hess, S. E.; Kogej, T.; Levin, M. D.; Marder, S. R.; McCord-Maughon, D.; Perry, J. W.; Röckel, H.; Rumi, M.; Subramaniam, G.; Webb, W. W.; Wu, X.-L.; Xu, C. *Science* **1998**, *281*, 1653–1656.
- (18) Reinhardt, B. A.; Brott, L. L.; Clarson, S. J.; Dillard, A. G.; Bhatt, J. C.; Kannan, R.; Yuan, L.; He, G. S.; Prasad, P. N. *Chem. Mater.* **1998**, *10*, 1863–1874.
- (19) Wang, C.-K.; Macak, P.; Luo, Y.; Ågren, H. *J. Chem. Phys.* **2001**, *114*, 9813–9820.
- (20) Denk, W.; Strickler, J. H.; Webb, W. W. *Science* **1990**, *248*, 73–76.
- (21) Xu, C.; Webb, W. W. In *Topics in Fluorescence Spectroscopy*; Lakowicz, J., Ed.; Nonlinear and Two-Photon-Induced Fluorescence; Plenum Press: New York, 1997; Vol. 5, pp 471–540.
- (22) Swofford, R. L.; McClain, W. M. *Chem. Phys. Lett.* **1975**, *34*, 455–460.
- (23) Birge, R. R. In *Ultrafast Laser Spectroscopy*; Kligler, D. S., Ed.; Academic Press: New York, 1983; pp 109–174.

- (24) Pond, S. J. K.; Rumi, M.; Levin, M. D.; Parker, T. C.; Beljonne, D.; Day, M. W.; Brédas, J.-L.; Marder, S. R.; Perry, J. W. *J. Phys. Chem. A* **2002**, *106*, 11470–11480.
- (25) Zhang, B.-J.; Jeon, S.-J. *Chem. Phys. Lett.* **2003**, *377*, 210–216.
- (26) Schmidt, R.; Tanielian, C.; Dunsbach, R.; Wolff, C. *J. Photochem. Photobiol., A* **1994**, *79*, 11–17.
- (27) Xu, C.; Webb, W. W. *J. Opt. Soc. Am. B* **1996**, *13*, 481–491.

Table 1. Relative Two-Photon Absorption Cross Sections Calculated Using Response Theory

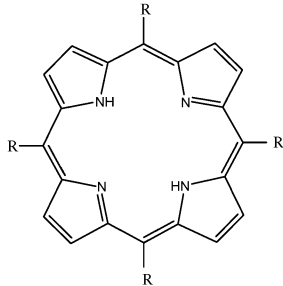
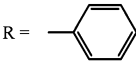
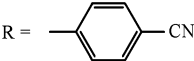

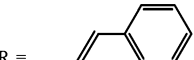
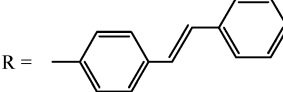
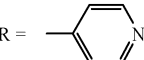
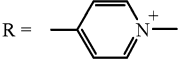
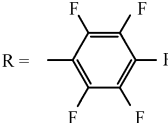
Molecule	Calculated Two-Photon Cross Sections ^a (Transition Energy, Irreducible Representation) ^b				
	Geometry = Unconstrained				
 TPP	1.37×10^4 (2.50, A'')	1.21×10^5 (3.51, A')	9.73×10^3 (3.97, A'')	1.77×10^4 (4.06, A')	C _s
	1.61×10^4 (2.49, A'')	1.42×10^5 (3.48, A')	1.17×10^4 (3.95, A'')	1.81×10^4 (4.05, A')	C _s
	1.46×10^4 (2.50, A)	1.29×10^5 (3.51, A)			C ₁
	1.88×10^4 (2.51, A'')	1.71×10^5 (3.55, A')	1.06×10^3 (3.81, A'')	1.32×10^4 (3.90, A')	C _s
	2.13×10^4 (2.50, A'')	1.98×10^5 (3.50, A')	1.14×10^4 (3.88, A'')	1.56×10^4 (3.98, A')	C _s
	1.35×10^4 (2.48, A'')	1.16×10^5 (3.46, A')	1.11×10^4 (3.96, A'')	1.82×10^4 (4.07, A')	C _s
 TMPyP	1.81×10^4 (2.51, A'')	1.63×10^5 (3.43, A')	1.34×10^4 (3.94, A'')	1.32×10^4 (4.06, A')	C _s
	1.79×10^4 (2.50, A'')	1.53×10^5 (3.44, A')	1.71×10^4 (3.98, A'')	1.33×10^4 (4.08, A')	C _s

Table 1. (Continued)

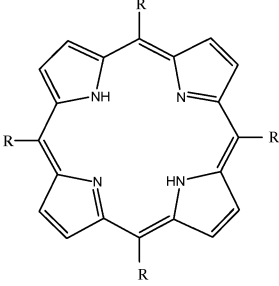
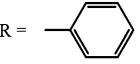
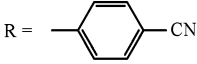

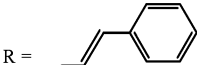
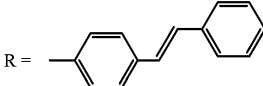
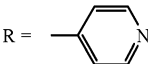
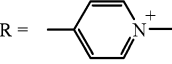
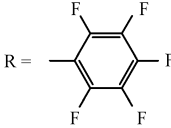
Molecule	Calculated Two-Photon Cross Sections (Transition Energy, Irreducible Representation)				
	Geometry = Flat				
 TPP	8.38×10^3 (2.29, B ₂)	2.42×10^5 (3.34, A₁)	7.89×10^1 (3.54, B ₂)	6.51×10^3 (3.64, A ₁)	C _{2v}
	8.61×10^3 (2.29, B ₂)	2.94×10^5 (3.32, A₁)	2.45×10^3 (3.49, B ₂)	9.33×10^3 (3.60, A ₁)	C _{2v}
	1.70×10^5 (3.89, B _{3g})	1.39×10^5 (4.23, A _g)	4.42×10^4 (4.34, B _{3g})	5.87×10^5 (4.53, A_g)	D _{2h}
	1.96×10^4 (2.10, B ₂)	2.14×10^6 (3.06, A₁)	4.13×10^4 (3.36, B ₂)	3.56×10^4 (3.54, A ₁)	C _{2v}
	1.34×10^4 (2.22, B ₂)	1.01×10^6 (3.26, A₁)	4.28×10^3 (3.36, B ₂)	7.19×10^5 (3.45, A ₁)	C _{2v}
	7.57×10^3 (2.33, B ₂)	1.38×10^5 (3.33, A₁)	3.29×10^3 (3.56, B ₂)	7.22×10^3 (3.69, A ₁)	C _{2v}
 TMPyP	1.04×10^4 (2.32, B ₂)	1.14×10^5 (3.10, A₁)	5.31×10^4 (3.43, B ₂)	2.71×10^4 (3.63, A ₁)	C _{2v}
	1.05×10^4 (2.49, B ₂)	1.16×10^5 (3.32, A₁)	5.35×10^1 (3.54, B ₂)	1.19×10^4 (3.76, A ₁)	C _{2v}

Table 1. (Continued)

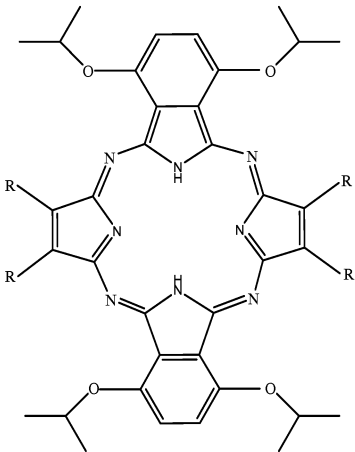
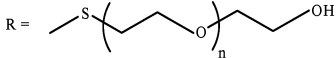
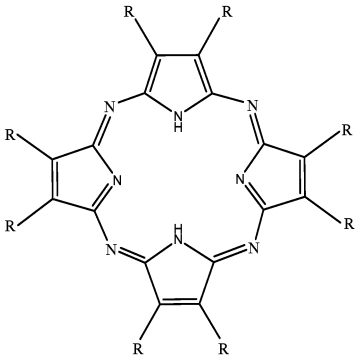
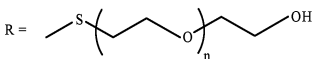
Molecule	Calculated Two-Photon Cross Sections (Transition Energy, Irreducible Representation)				
 <p style="text-align: center;">Porphyrzine I^c</p>					
	5.78×10^5 (1.99, A'')	5.17×10^6 (2.78, A')	2.87×10^4 (3.38, A')	1.18×10^5 (3.38, A'')	Unconstrained <i>C_s</i>
	4.26×10^5 (2.12, B ₂)	3.01×10^6 (2.76, A₁)	1.10×10^5 (2.99, A ₁)	3.00×10^5 (3.00, B ₂)	Flat <i>C_{2v}</i>
 <p style="text-align: center;">Porphyrzine II^c</p>					
	1.61×10^5 (2.58, A'')	5.38×10^4 (3.23, A'')	2.06×10^4 (3.24, A')	7.07×10^5 (3.27, A')	Unconstrained <i>C_s</i>
	6.49×10^6 (3.03, A_g)	1.15×10^6 (3.62, A _g)	1.82×10^{-1} (5.19, B _g)	6.97×10^1 (5.41, B _g)	Flat <i>C_{2h}</i>

Table 1. (Continued)

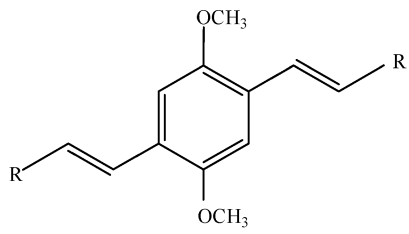
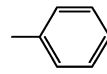
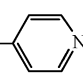
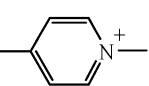
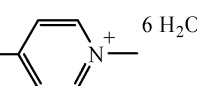
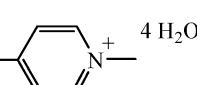
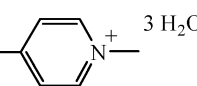
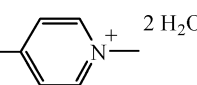
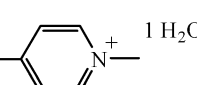
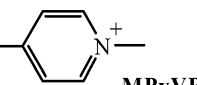
Molecule	Calculated Two-Photon Cross Sections (Transition Energy, Irreducible Representation)				
 Geometry = Unconstrained					
R = 	8.41 x 10 ³ (4.89, A _g)	2.88 x 10⁴ (5.69, A _g)	2.71 x 10 ¹ (8.20, B _g)	1.30 x 10 ² (8.67, B _g)	C _{2h}
R = 	1.76 x 10 ⁴ (4.99, A _g)	2.65 x 10⁴ (5.72, A _g)	1.11 x 10 ³ (5.76, B _g)	5.16 x 10 ² (7.31, B _g)	C _{2h}
R ^{d,e} = 	1.74 x 10 ⁵ (2.56, A _g)	3.04 x 10⁵ (3.24, A _g)			C _i
R = 	1.06 x 10⁶ (4.71, A _g)	1.26 x 10 ⁵ (5.45, A _g)			C _i
R = 	1.03 x 10⁶ (4.74, A _g)	4.47 x 10 ⁴ (5.48, A _g)	1.09 x 10 ² (8.12, B _g)	1.36 x 10 ⁰ (8.41, B _g)	C _{2h}
R = 	1.28 x 10⁶ (4.70, A _g)	5.31 x 10 ⁴ (5.48, A _g)			C _i
R = 	1.59 x 10⁶ (4.66, A _g)	5.83 x 10 ⁴ (5.48, A _g)			C _i
R = 	2.13 x 10⁶ (4.60, A _g)	2.28 x 10 ⁵ (5.51, A _g)	1.00 x 10 ² (8.11, B _g)	1.08 x 10 ¹ (8.31, B _g)	C _{2h}
R =  MPyVB	2.70 x 10⁶ (4.50, A _g)	1.52 x 10 ⁵ (5.51, A _g)	7.74 x 10 ¹ (8.08, B _g)	2.03 x 10 ⁰ (8.48, B _g)	C _{2h}

Table 1. (Continued)

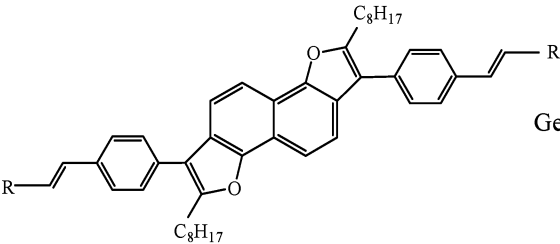
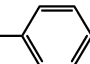
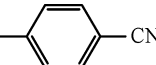
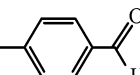
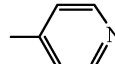
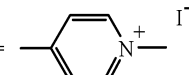
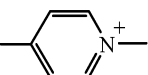
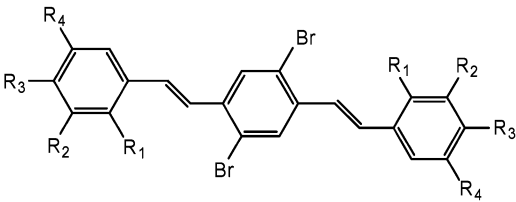
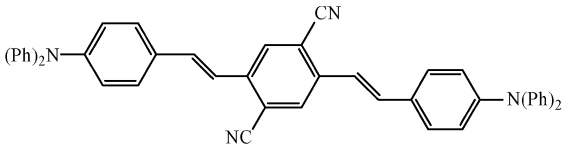
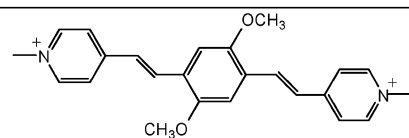
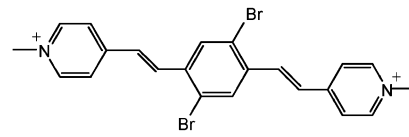
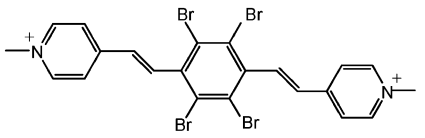
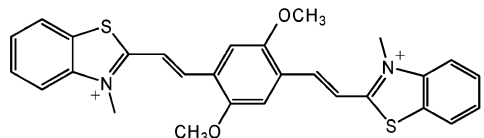
Molecule	Calculated Two-Photon Cross Sections (Transition Energy, Irreducible Representation)				
 Geometry = Unconstrained					
R = 	1.58 x 10 ¹ (4.16, B)	9.41 x 10 ³ (4.21, A)	4.38 x 10 ⁰ (4.48, B)	5.87 x 10⁴ (5.43, A)	C ₂
R = 	4.61 x 10 ² (4.02, B)	1.37 x 10⁵ (4.07, A)	2.88 x 10 ⁰ (4.47, B)	1.00 x 10 ⁵ (5.29, A)	C ₂
R = 	6.06 x 10 ² (4.00, B)	1.53 x 10⁵ (4.05, A)	4.04 x 10 ⁰ (4.47, B)	3.21 x 10 ⁴ (5.26, A)	C ₂
R = 	2.25 x 10 ² (4.18, B)	6.94 x 10⁴ (4.23, A)	4.79 x 10 ⁰ (4.48, B)	3.75 x 10 ⁴ (5.46, A)	C ₂
R ^{d,e} = 	1.43 x 10 ⁵ (2.67, A _g)	1.54 x 10⁵ (3.36, A_g)			C _i
R = 	3.06 x 10 ⁶ (3.49, A _g)	2.78 x 10⁶ (4.68, A_g)			C _i
					
R ₁ = R ₃ = OCH ₃ ^e R ₂ = R ₄ = H	1.78 x 10 ⁵ (4.78, A _g)	8.65 x 10 ⁴ (5.84, A _g)	1.57 x 10 ³ (6.46, B _g)	2.47 x 10⁶ (7.37, B_g)	C _{2h}
R ₁ = R ₄ = H ^e R ₂ = R ₃ = OCH ₃	6.07 x 10⁵ (4.75, A_g)	1.01 x 10 ⁵ (5.69, A _g)	1.49 x 10 ³ (6.50, B _g)	4.81 x 10 ⁵ (7.43, B _g)	C _{2h}
R ₁ = R ₃ = H ^e R ₂ = R ₄ = OCH ₃	1.35 x 10 ⁵ (5.00, A)	3.21 x 10 ⁴ (5.49, A)	1.68 x 10 ⁶ (6.64, A)	9.28 x 10⁷ (6.78, A)	C ₂
R ₁ = H ^e R ₂ = R ₃ = R ₄ = OCH ₃	5.54 x 10 ⁵ (4.79, A _g)	1.52 x 10 ⁴ (5.56, A _g)	8.73 x 10 ⁶ (6.51, A _g)	8.88 x 10⁷ (6.54, A_g)	C _i

Table 1. (Continued)

Molecule	Calculated Two-Photon Cross Sections (Transition Energy, Irreducible Representation)		
	1.21 x 10⁶ (4.52, A _g)	8.23 x 10 ⁴ (5.40, A _g)	C _i

^a In atomic units. Data shown correspond to 30δ (see eq 1). For a given molecule, the transition with the largest cross section is shown in boldface. ^b Transition energies in eV. As explained in the section on computational methods, the calculated transition energies are larger than those that would be experimentally observed. For each molecule, we identify the point group used and the corresponding irreducible representation to which the given transition transforms. ^c Experiments were performed using molecules where $n = 2$. Computations were performed using $n = 1$. ^d Although arguably “unrealistic”, this is included simply to show the effect of a tightly bound counterion. ^e Calculated using the 3-21G basis set.

Table 2. Singlet Oxygen Quantum Yields, ϕ_{Δ} , for a Series of Cationic Divinyl Benzenes^a

Molecule	$\phi_{\Delta}(\text{water})$
	0.02
	0.03
	0
	0.01

^a Recorded in air-saturated water. Data were recorded using perinaphthenone sulfonic acid as the standard ($\phi_{\Delta} = 1.0$).^{30,31} The counterion was CH_3SO_4^- .

produced upon one-photon excitation (i.e., irrespective of the method by which initial excitation is achieved, Kasha's rule will be obeyed and the lowest excited singlet state will be formed with unit efficiency). Then, to obtain a relative value for the absorption cross section, it is only necessary to normalize the observed singlet oxygen phosphorescence intensities by the singlet oxygen quantum yields for these respective molecules. The latter are readily obtained in independent one-photon experiments performed against a singlet oxygen standard.

This method of using singlet oxygen phosphorescence intensities to quantify two-photon absorption cross sections has a number of advantages. As outlined in the Results section, because singlet oxygen has a comparatively long lifetime, the signal of interest is temporally displaced from the undesired signal associated with pulsed laser irradiation (i.e., scattered light). Second, irrespective of the molecule irradiated, the signal detected always has the same spectral profile (i.e.,

the discrete singlet oxygen emission spectrum^{28,29}). Thus, the number of photons emitted over this narrow bandwidth is readily quantified without the need for molecule-dependent spectral corrections. Finally, because the effect of solvent on radiative transitions in singlet oxygen is now thoroughly understood,^{5,12,13} it is possible to quantify absorption cross sections in a range of solvents upon comparison to data recorded from the standard **CNPhVB** dissolved in toluene (see Supporting Information, Appendix 3).

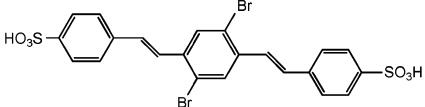
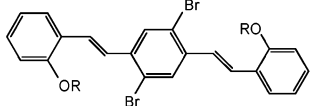
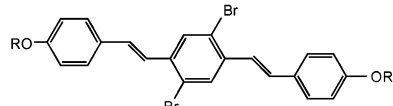
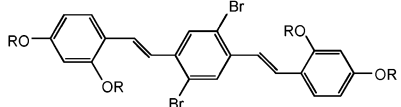
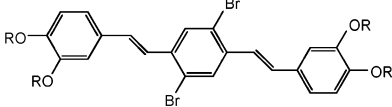
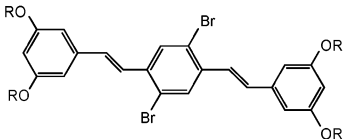
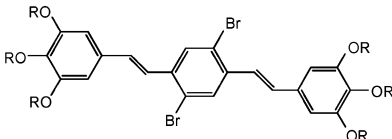
Singlet Oxygen Sensitizers. Structures of the molecules used as singlet oxygen sensitizers are shown in Tables 1–3.

5,10,15,20-Tetrakis(*N*-methyl-4-pyridyl)-21*H*,23*H*-porphine, **TMPyP**, was purchased from Aldrich as the tetra-*p*-tosylate salt and used as received. In an independent one-photon experiment, we

(28) Macpherson, A. N.; Truscott, T. G.; Turner, P. H. *J. Chem. Soc., Faraday Trans.* **1994**, *90*, 1065–1072.

(29) Wessels, J. M.; Rodgers, M. A. J. *J. Phys. Chem.* **1995**, *99*, 17586–17592.

Table 3. Singlet Oxygen Quantum Yields, ϕ_{Δ} , for a Series of Distyryl Benzenes^a

Molecule ^b	$\phi_{\Delta}(\text{toluene})$	$\phi_{\Delta}(\text{water})^c$
	0.22	
	0.33	
	0.35	
	0.32	0.20
	0.26	0.14
	0.18	0.10
	0.35	0.14

^a Recorded in air-saturated solvents. Data in water were recorded using perinaphthenone sulfonic acid as the standard ($\phi_{\Delta} = 1.0$),^{30,31} whereas data in toluene were recorded using perinaphthenone as the standard ($\phi_{\Delta} = 1.0$).²⁶ Errors are $\pm 10\%$. ^b R = $-(\text{CH}_2\text{CH}_2\text{O})_2\text{CH}_2\text{CH}_2\text{OCH}_3$. ^c Although these values were obtained using reasonably low laser energies, we cannot exclude the possibility that the data are nevertheless still influenced by the putative quencher discussed in the text. In this regard, the values shown may be slightly smaller than the true values of $\phi_{\Delta}(\text{water})$ for these sensitizers.

ascertained that, in air-saturated water, this molecule produces singlet oxygen with a quantum yield, ϕ_{Δ} , of 0.77 ± 0.04 (determined against a singlet oxygen phosphorescence signal produced upon irradiation of perinaphthenone sulfonic acid with $\phi_{\Delta} = 1.0$).^{30,31} Although our quantum yield of 0.77 is larger than that reported by Gensch et al. ($\phi_{\Delta} = 0.58 \pm 0.05$),³² it is consistent with that reported by Verlhac et al. ($\phi_{\Delta} = 0.74$).³³

2,5-Dimethoxy-1,4-bis(2-[*N*-methylpyridinium-4-yl]vinyl)benzene, **MPyVB**, was prepared using an approach similar to that of Iwase et

al.³⁴ 2,5-Dibromo-1,4-bis(2-[*N*-methylpyridinium-4-yl]vinyl)benzene methyl sulfate, **BrPyVB**, was similarly prepared, in this case using a Horner–Wadsworth–Emmons reaction between [2,5-dibromo-4-(diethoxyphosphorylmethyl)benzyl]phosphoric acid diethylester and pyridine-4-carbaldehyde.^{7,34,35} The oligo(ethylene glycol)-substituted distyryl benzenes were likewise prepared using the analogous Horner–

(30) Nonell, S.; Gonzalez, M.; Trull, F. R. *Afinidad L* **1993**, 448, 445–450.

(31) Marti, C.; Jürgens, O.; Cuenca, O.; Casals, M.; Nonell, S. *J. Photochem. Photobiol., A* **1996**, 97, 11–18.

(32) Gensch, T.; Viappiani, C.; Braslavsky, S. E. *J. Am. Chem. Soc.* **1999**, 121, 10573–10582.

(33) Verlhac, J. B.; Gaudemer, A.; Kraljic, I. *Nouv. J. Chim.* **1984**, 8, 401–406.

(34) Iwase, Y.; Kamada, K.; Ohta, K.; Kondo, K. *J. Mater. Chem.* **2003**, 13, 1575–1581.

(35) Blum, J.; Zimmerman, M. *Tetrahedron* **1972**, 28, 275–280.

Wadsworth–Emmons reaction, in this case with the appropriate oligo-(ethylene glycol)-substituted benzaldehyde. The latter were prepared from the corresponding hydroxybenzaldehyde in a reaction with the tosylated triethylene glycol monomethyl ether using K_2CO_3 as the base.

2,5-Dicyano-1,4-bis(2-(4-diphenylaminophenyl)vinyl)benzene, **CNPhVB**, was synthesized via a Horner–Wadsworth–Emmons reaction in an approach that has been outlined elsewhere.^{7,24} The porphyrazine I, whose synthesis is published,³⁶ was provided by Professor B. M. Hoffman (Northwestern University).

Computational Methods. Features of our ab initio computational approach have been described previously.⁸ Briefly, calculations were performed with the DALTON program package,³⁷ using response theory to obtain the two-photon absorption cross sections. For this application, the principal attribute of response theory is the ability to obtain the two-photon cross section in one calculation in which the virtual state is effectively described as a linear combination of all states of the molecule.³⁸ Thus, we explicitly avoid the limitations of a traditional sum-over-states calculation^{39–41} in which the accuracy of the result can be compromised if one or more key states of the molecule are neglected.

In our approach, the matrix elements for a two-photon electric dipole transition, $S_{\alpha\beta}$, were calculated through a residue of the quadratic response function.³⁸ The molecule-averaged two-photon transition moment for linearly polarized light, δ , which is proportional to the absorption cross section, was then expressed in terms of these matrix elements, summed over the molecular axes (eq 1, where $\alpha = x, y, z$ and $\beta = x, y, z$).^{40,42}

$$\delta = \frac{1}{30} \sum_{\alpha, \beta} (2S_{\alpha, \alpha} S_{\beta, \beta} + 4S_{\alpha, \beta} S_{\beta, \alpha}) \quad (1)$$

Except where otherwise noted, the response calculations were carried out using the 6-31G* basis set.

Prior to the response calculations, the geometries of the molecules, including the molecules with surrounding solvent, were optimized using a number of approaches available in the Gaussian 98 program,⁴³ including an approach based on density functional theory. For a given molecule, calculated two-photon transition energies and absorption cross sections can depend significantly on the geometry used.⁸ This is indeed to be expected, particularly when the geometric variable influences the extent of conjugation in the system. With the comparatively large molecules used in our work, for which a number of conformation-dependent local minima exist, the “optimum” geometry obtained can

be very sensitive to the optimization method used. For these reasons, when performing the geometry optimizations for a given series of molecules, we tried to be consistent in an attempt to ensure that relative changes in the cross sections would be accurate. We also examined the effect of constraining the molecule to a specific geometry (i.e., a planar system) and comparing the results obtained to those obtained using an unconstrained geometry.

The absorption cross section obtained from the response theory computation is in atomic units. To compare the latter with experimental data, it is necessary to convert to a number with the units of $cm^4 s photon^{-1} molecule^{-1}$. Among other things, this transformation involves multiplication by a band shape function that can vary from one molecule to the next.^{8,44–46} For our present application, in which we want only to focus on relative changes in the magnitude of the absorption cross section, we have opted to report numbers in atomic units.

It is likewise important to recognize that, due to the size of the systems involved, the calculations were performed on the uncorrelated Hartree–Fock level. Moreover, unless explicitly indicated, the effect of solvent has not been included. As a consequence, the calculated transition energies are generally larger than those that would be experimentally observed from solution phase systems. Although this is a general problem common to such computations,^{19,47} the calculated differences between transition energies should be reasonably accurate.

Results and Discussion

Computations. It has been demonstrated, both through our own work⁸ and through the work of others,^{19,45} that ab initio computations based on response theory can yield relative values for the two-photon absorption cross sections of large molecules that are reasonably accurate. From our perspective, such computations have become indispensable, not just as an aid in the interpretation of experimental data but as a tool to predict which molecules are likely to be worth the often extensive efforts required for their synthesis.

For the present study, we set out to examine several conjugated pi systems that are either known to be, or that could be, reasonable water-soluble singlet oxygen sensitizers. As a starting point, it was anticipated that, because of its positive charge, an *N*-methylpyridyl substituent could not only impart significant water solubility but also contribute to the polarization of the pi system and thus result in large transition dipole moments. Indeed, the pertinent *N*-methylpyridyl-substituted porphyrin, **TMPyP**, is known to be an efficient water-soluble singlet oxygen sensitizer.^{9,33,48} On the basis of our success with distyryl benzenes and difuranonaphthalenes as two-photon sensitizers in toluene,^{7,8} we set out to examine the potential effect of the *N*-methylpyridyl group on these chromophores as well. Our initial concern was simply to examine the extent to which specific substituents influenced the two-photon absorption cross section. The results of these calculations are shown in Table 1.

A. Porphyrins. In our first series of calculations, we examined the extent to which substituents in the meso position of the porphyrin influence the cross section. Keeping in mind our caveats about the effects of molecular conformation (see Computational Methods), our calculations indicate that the effect

(36) Ehrlich, L. A.; Skrdla, P. J.; Jarrell, W. K.; Sibert, J. W.; Armstrong, N. R.; Saavedra, S. S.; Barrett, A. G. M.; Hoffman, B. M. *Inorg. Chem.* **2000**, *39*, 3963–3969.

(37) Helgaker, T.; Jensen, H. J. A.; Jørgensen, P.; Olsen, J.; Ruud, K.; Ågren, H.; Bak, K. L.; Bakken, V.; Christiansen, O.; Coriani, S.; Dahle, P.; Dalgaard, E. K.; Enevoldsen, T.; Fernandez, B.; Haettig, C.; Hald, K.; Halkier, A.; Heiberg, H.; Hettner, H.; Jonsson, D.; Kirpekar, S.; Kobayashi, R.; Koch, H.; Mikkelsen, K. V.; Norman, P.; Packer, M. J.; Pedersen, T. B.; Ruden, T. A.; Sanchez, A.; Sauer, T.; Sauer, S. P. A.; Schimmelpennig, B.; Sylvester-Hvid, K. O.; Taylor, P. R.; Vahtras, O. *Dalton, a molecular electronic structure program*, release 1.2 (2001); see <http://www.kjemi.uio.no/software/dalton/dalton.html>.

(38) Olsen, J.; Jørgensen, P. *J. Chem. Phys.* **1985**, *82*, 3235–3264.

(39) Bhawalkar, J. D.; He, G. S.; Prasad, P. N. *Rep. Prog. Phys.* **1996**, *59*, 1041–1070.

(40) Birge, R. R.; Pierce, B. M. *J. Chem. Phys.* **1979**, *70*, 165–178.

(41) Kogej, T.; Beljonne, D.; Meyers, F.; Perry, J. W.; Marder, S. R.; Brédas, J. L. *Chem. Phys. Lett.* **1998**, *298*, 1–6.

(42) McClain, W. M. *J. Chem. Phys.* **1971**, *55*, 2789–2796.

(43) Frisch, M. J.; Trucks, G. W.; Schlegel, H. B.; Scuseria, G. E.; Robb, M. A.; Cheeseman, J. R.; Zakrewski, V. G.; Montgomery, J. A., Jr.; Stratmann, R. E.; Burant, J. C.; Dapprich, S.; Millam, J. M.; Daniels, A. D.; Kudin, K. N.; Strain, M. C.; Farkas, O.; Tomasi, J.; Barone, V.; Cossi, M.; Cammi, R.; Mennucci, B.; Pomelli, C.; Adamo, C.; Clifford, S.; Ochterski, J.; Petersson, G. A.; Ayala, P. Y.; Cui, Q.; Morokuma, K.; Malick, D. K.; Rabuck, A. D.; Raghavachari, K.; Foresman, J. B.; Ortiz, J. V.; Baboul, A. G.; Cioslowski, J.; Stefanov, B. B.; Liu, G.; Liashenko, A.; Piskorz, P.; Komaromi, I.; Gomperts, R.; Martin, R. L.; Fox, D. J.; Keith, T.; Al-Laham, M. A.; Peng, C. Y.; Nanayakkara, A.; Challacombe, M.; Gill, P. M. W.; Johnson, B.; Chen, W.; Wong, M. W.; Andres, J. L.; Gonzalez, C.; Head-Gordon, M.; Replogle, E. S.; Pople, J. A. *Gaussian 98*, revision A.7; Gaussian Inc.: Pittsburgh, PA, 1998.

(44) Birge, R. R.; Bennett, J. A.; Pierce, B. M.; Thomas, T. M. *J. Am. Chem. Soc.* **1978**, *100*, 1533–1539.

(45) Norman, P.; Luo, Y.; Ågren, H. *J. Chem. Phys.* **1999**, *111*, 7758–7765.

(46) Peticolas, W. L. *Ann. Rev. Phys. Chem.* **1967**, *18*, 233–260.

(47) Poulsen, T. D.; Ogilby, P. R.; Mikkelsen, K. V. *J. Chem. Phys.* **2001**, *115*, 7843–7851.

(48) Zebger, I.; Snyder, J. W.; Andersen, L. K.; Poulsen, L.; Gao, Z.; Lambert, J. D. C.; Kristiansen, U.; Ogilby, P. R. *Photochem. Photobiol.* **2004**, *79*, 319–322.

of such substituents on the two-photon absorption cross section is not particularly pronounced. Indeed, even if we impose the constraint of a flat molecule in which the extent of pi conjugation is maximized, we find that such a substituent change has only a modest effect. It is important to note that this observation is based on data from what appears to be the same transition in each of the molecules examined (i.e., similar transition energy, same symmetry).

It is specifically important to note that, upon examination of the charged *N*-methylpyridyl derivative (i.e., a system with no counterion), the cross section calculated is not significantly different from that calculated for tetraphenyl porphine, **TPP**. This result is consistent with experimental data, albeit in different solvents, in which two-photon cross sections measured for **TPP** in toluene over the range ~1100–1400 nm are similar to those of **TMPyP** in water.⁹

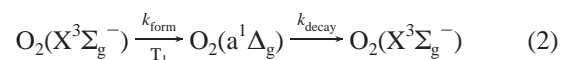
These conclusions about the effect of substituent changes on a phenyl group at the meso position of the porphyrin ring are also consistent with the observation that the one-photon absorption spectra of these molecules are all very similar.^{49,50}

B. Porphyrazines. To continue our study on the influence that a given site in the porphyrin framework may have on the two-photon absorption cross section, we next considered possible changes in the core of the macrocycle. In the porphyrazine, or tetraazaporphyrin, ring structure, the meso positions of the porphyrin macrocycle contain nitrogen not carbon. For the molecules shown in Table 1, we calculate a two-photon cross section that is over 1 order of magnitude larger than that calculated for the substituted porphyrins. To put these numbers in perspective, we estimate that, for porphyrazine I in an unconstrained geometry, the calculations correspond to an absorption cross section of $\sim 900 \times 10^{-50} \text{ cm}^4 \text{ s photon}^{-1} \text{ molecule}^{-1}$. Recent experiments document that porphyrazines can indeed have two-photon cross sections that are significantly larger than those in porphyrins.^{9,51}

C. Divinylbenzenes and Difuranonaphthalenes. In calculations performed on difuranonaphthyl and divinyl benzene frameworks, we find a pronounced substituent effect on the two-photon absorption cross section, including the effect expected upon placing the charged *N*-methylpyridyl moiety at the periphery of the pi system. With respect to the latter, it is also reassuring to note that as we mitigate the positive charge either with a counterion or with water solvent molecules, the absorption cross section changes accordingly. The results of our calculations are also in general agreement with experimental data. In this case, we note that Iwase et al.³⁴ have reported a maximum cross section for **MPyVB** of $(350 \pm 50) \times 10^{-50} \text{ cm}^4 \text{ s photon}^{-1} \text{ molecule}^{-1}$. This cross section is roughly a factor of 15 times larger than the cross section of $\sim 20 \times 10^{-50} \text{ cm}^4 \text{ s photon}^{-1} \text{ molecule}^{-1}$ reported for **TPP** at ~765 nm.⁹ As seen in Table 1, our calculations are consistent with this relative change in cross section.

Experiments. With our computational results in mind, we set out to perform a series of experiments to produce and detect singlet oxygen upon two-photon excitation of a sensitizer dissolved in water.

A. Time-Resolved Singlet Oxygen Signal. Pertinent events in the triplet state photosensitized production of singlet oxygen are shown in eq 2.



Upon pulsed laser excitation of a sensitizer, followed by equally rapid formation of the sensitizer triplet state, T₁, the concentration of singlet oxygen will evolve in time according to eq 3,

$$[\text{O}_2(\text{a}^1\Delta_g)]_t = \frac{k_{\text{form}}[\text{O}_2(\text{X}^3\Sigma_g^-)]}{k_{\text{decay}} - k_{\text{T}}} [\text{T}_1]_0 (e^{-k_{\text{T}}t} - e^{-k_{\text{decay}}t}) \quad (3)$$

where k_{T} is the rate constant that expresses all channels for the decay of the triplet state, including the oxygen-dependent bimolecular channel $k_{\text{form}}[\text{O}_2(\text{X}^3\Sigma_g^-)]$, and $[\text{T}_1]_0$ is the concentration of triplet states produced at “time = 0”.

Because the concentration of oxygen in water is comparatively low ($\sim 2.5 \times 10^{-4} \text{ M}$ in an air-saturated solution⁵²) and because the rate constant for singlet oxygen decay in water is comparatively large, the rate constant for overall triplet state decay, k_{T} , will be roughly equivalent to k_{decay} in a typical aqueous system. As a consequence, the time evolution of the singlet oxygen signal observed in a time-resolved phosphorescence experiment should appear as the difference of two exponential functions, showing distinct rising and falling components (eq 3). This contrasts with what is typically observed in experiments performed in hydrocarbon solvents, for example, where $k_{\text{T}} > k_{\text{decay}}$ and eq 3 reduces to a function with a single-exponential decay.

Upon 780 nm pulsed laser irradiation of a water solution containing **TMPyP**, we were able to detect a time-resolved emission signal at 1270 nm (Figure 1).

The data shown in Figure 1 can be assigned to singlet oxygen phosphorescence on the basis of the following points: (1) The $\text{a}^1\Delta_g \rightarrow \text{X}^3\Sigma_g^-$ emission has a band maximum at ~1270 nm,^{28,29} and our data were recorded using a 1270 nm interference filter (fwhm = 50 nm) placed between the sample and the detector. (2) Both the kinetics and the intensity of the signal observed were sensitive to the oxygen concentration in the sample and behaved as expected on the basis of eq 3. The signal was not observed in the absence of oxygen. (3) For a sample prepared with a given oxygen concentration, the rate of triplet state sensitizer decay was quantified in an independent time-resolved absorption experiment. The rate constant thus obtained, k_{T} , was then used as a parameter in eq 3 which, in turn, was used in an iterative fitting routine to obtain k_{decay} from the 1270 nm emission signal. Values of k_{decay} obtained from such fits corresponded to those expected for the decay of singlet oxygen in H₂O [i.e., ($\sim 3.5 \mu\text{s}$)⁻¹]. (4) Values of k_{decay} obtained from corresponding fits of eq 3 to data recorded in D₂O likewise yielded the value expected for the decay of singlet oxygen in this particular solvent [i.e., ($\sim 68 \mu\text{s}$)⁻¹].⁵³

On the basis of the following points, we conclude that the singlet oxygen signals observed upon irradiation of aqueous solutions of **TMPyP** at wavelengths over the range 765–845 nm are a consequence of **TMPyP** excitation in a two-photon

(49) Thomas, D. W.; Martell, A. E. *J. Am. Chem. Soc.* **1956**, *78*, 1338–1343.

(50) Gouterman, M. In *The Porphyrins*; Dolphin, D., Ed.; Academic Press: New York, 1978; Vol. 3, pp 1–165.

(51) Drobizhev, M.; Karotki, A.; Kruk, M.; Mamardashvili, N. Z.; Rebane, A. *Chem. Phys. Lett.* **2002**, *361*, 504–512.

(52) Battino, R., Ed. *IUPAC Solubility Data Series. Volume 7: Oxygen and Ozone*; Pergamon Press: Oxford, 1981.

(53) Ogilby, P. R.; Foote, C. S. *J. Am. Chem. Soc.* **1983**, *105*, 3423–3430.

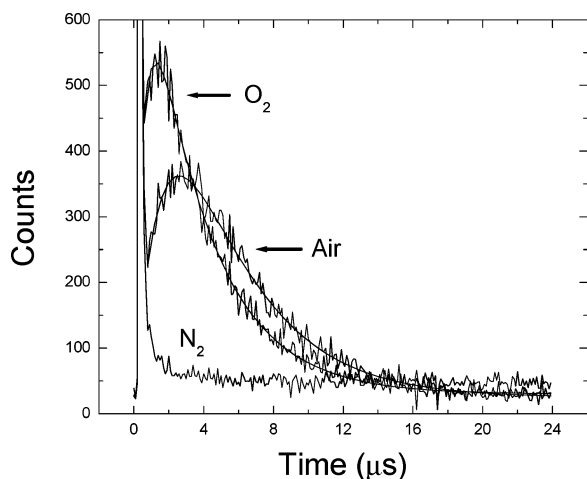


Figure 1. Time-resolved 1270 nm emission signals recorded upon 780 nm irradiation of an aqueous solution containing 2×10^{-4} M **TMPyP**. Data recorded from oxygen-saturated, air-saturated, and nitrogen-saturated solutions are shown. A 100 ns sampling window was used on the photon counter. For each of the points used to construct the decay trace, data were accumulated for 60 s which, at a laser repetition rate of 1 kHz, corresponds to 60 000 laser pulses. Under these conditions, and using two separate sampling windows, it thus took 2 h to record each 24 μ s trace shown. A laser energy of 140 μ J/pulse was used with a beam waist of 600 μ m. The spike that precedes the signal assigned to singlet oxygen derives from a combination of scattered laser light and sensitizer luminescence. Superimposed on each kinetic trace is the result of a fit of eq 3 to the data.

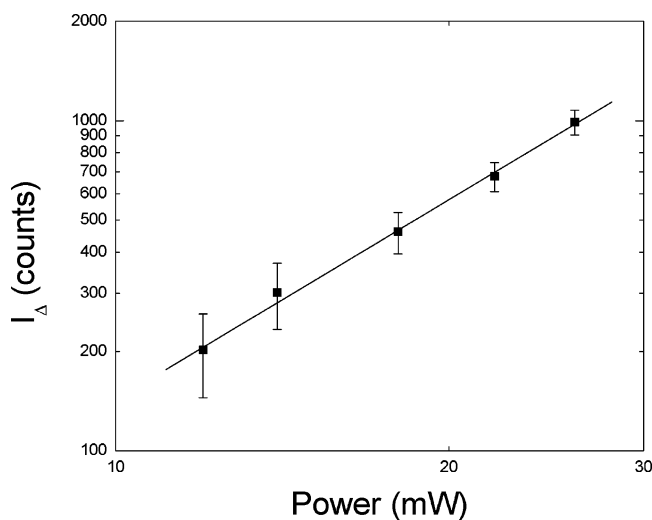


Figure 2. Double logarithmic plot of the singlet oxygen phosphorescence intensity, I_{Δ} , against the average laser power incident on the sample. These data were recorded upon 780 nm irradiation of an aqueous solution of **TMPyP** at a repetition rate of 1 kHz. Therefore, an incident power of 20 mW, for example, corresponds to 20 μ J/pulse (beam waist = 300 μ m). The solid line is a linear fit to the data and has a slope of 2.0 ± 0.3 . Values of I_{Δ} were obtained by integrating the time-resolved singlet oxygen signals.

process: (1) As shown in Figure 2, the intensity of the signals scales according to the square of the intensity of the irradiating laser. (2) **TMPyP** does not have a resonant, one-photon transition at the irradiation wavelengths used in the two-photon experiments (see Figure 3). (3) The emission signal at 1270 nm was not observed upon irradiation of **TMPyP**-free water. (4) Under conditions in which irradiation yielded singlet oxygen signals, we were also able to detect **TMPyP** fluorescence at 680 nm. The intensity of the latter likewise scaled according to the square of the intensity of the irradiating laser.

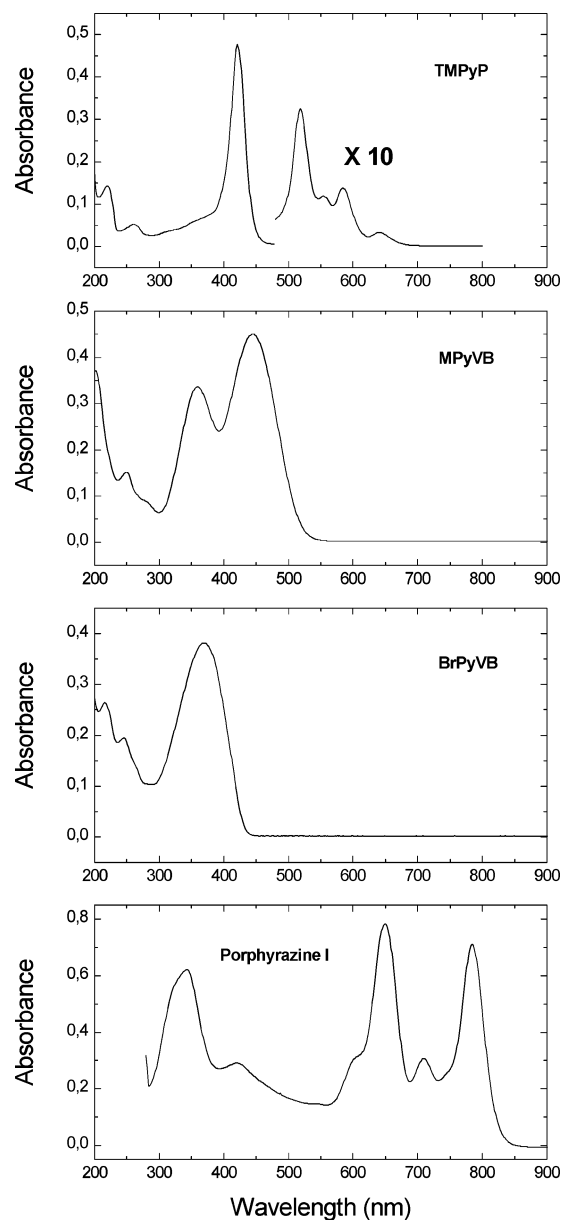


Figure 3. One-photon absorption spectra of sensitizers used in this study. (a) **TMPyP** in H_2O . (b) **MPyVB** in H_2O . (c) **BrPyVB** in H_2O . (d) Porphyrazine I in toluene.

It is important to note in Figure 1 that, for samples containing oxygen, the signal decays to a baseline which is different from that recorded in the absence of oxygen. Specifically, in the nitrogen-saturated sample, a long-lived 1270 nm emission is observed. Given that we are detecting extremely weak signals in this experiment (i.e., the quantum yield of singlet oxygen phosphorescence is $\sim 3 \times 10^{-7}$), it is reasonable to suggest that this long-lived emission detected in the absence of oxygen is **TMPyP** phosphorescence. Of course, in the presence of oxygen, this emission is quenched and, thus, cannot be observed once the singlet oxygen signal decays. This same phenomenon was also observed upon one-photon excitation of **TMPyP** in H_2O .

It is also important to note in Figure 1 that the singlet oxygen signal is temporally displaced relative to the signal that derives from more rapid events coincident with the laser pulse (i.e., scattered laser light, sensitizer fluorescence). The ability to discriminate between these signals can have important ramifica-

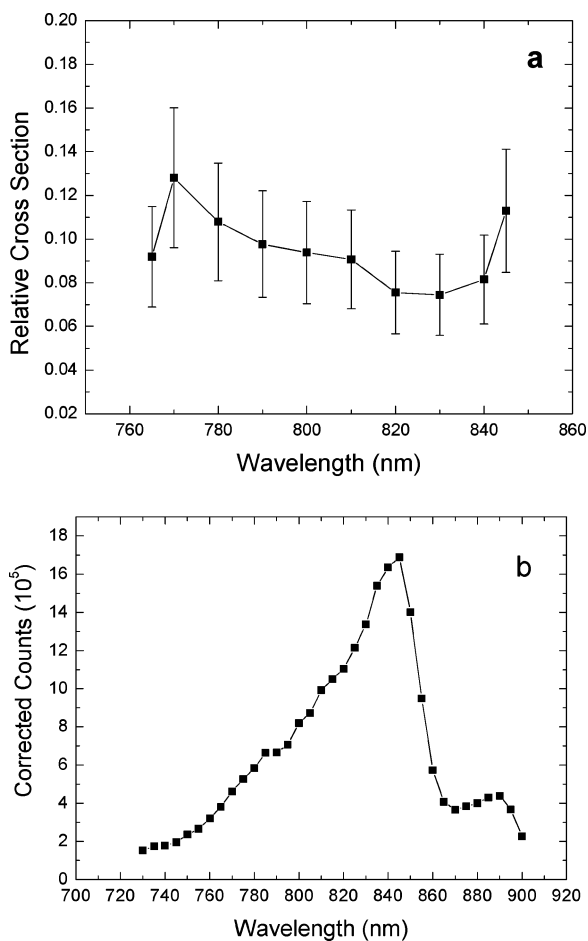


Figure 4. (a) Plot of the relative absorption cross section against the irradiation wavelength for the two-photon excitation of **TMPyP** in water. The data were obtained using the phosphorescence of singlet oxygen as a probe, and for data recorded at a given irradiation wavelength, the intensity of the signals always scaled according to the square of the laser intensity. The error bars shown ($\pm 25\%$) include the uncertainty that arises in the comparison to the standard **CNPhVB**. (b) Two-photon excitation spectrum of the standard molecule **CNPhVB** in toluene.

tions when creating singlet oxygen based images of a sample or when using singlet oxygen phosphorescence to quantify the two-photon absorption cross section of the sensitizer.

B. Relative TMPyP Absorption Cross Section. For our present study, we would like to ascertain if **TMPyP** is indeed a molecule that has an acceptably large two-photon absorption cross section. To this end, we compared the intensity of the two-photon **TMPyP** photosensitized singlet oxygen signal to the intensity of the singlet oxygen signal obtained upon two-photon irradiation of **CNPhVB**. The two-photon absorption profile of **CNPhVB** we obtained in toluene is shown in Figure 4. Although values reported for the absolute cross section of **CNPhVB** at its peak maximum cover a large range,^{17,24,25} the data indicate that the molecule has a comparatively large two-photon cross section (e.g., $(1890 \pm 280) \times 10^{-50} \text{ cm}^4 \text{ s photon}^{-1} \text{ molecule}^{-1}$ at $\sim 840 \text{ nm}$).²⁴

The two-photon absorption profile we obtain for **TMPyP** in H₂O is shown in Figure 4. Over the wavelength range examined, we determined that the band maximum for **CNPhVB** at 845 nm is ~ 8 times larger than the maximum for **TMPyP** at 770 nm. This is consistent with the calculations shown in Table 1, where the maximum cross section for **CNPhVB** is expected to be ~ 7 times larger than that of **TMPyP**.

C. Other Singlet Oxygen Sensitizers. In an attempt to establish a broad-based collection of water-soluble two-photon singlet oxygen sensitizers, we explored the option of using sensitizers other than **TMPyP**.

(i) ***N*-Methylpyridyl-Substituted Divinyl Benzenes.** On the basis of our success with the use of distyryl benzenes as two-photon sensitizers in toluene,^{7,8} we set out to prepare water-soluble variants of these systems. Moreover, given our success with **TMPyP**, we opted to first focus on the use of *N*-methylpyridyl moieties which, as a functional group carrying a positive charge, could not only impart significant water solubility but also potentially contribute to large transition dipole moments.

When paired with cationic *N*-methylpyridyl groups placed on the ends of a conjugated pi system, electron donating groups placed in the middle of the pi system should enhance polarization effects and result in a larger transition moment. Our computations indeed indicate that a dimethoxy-1,4-bis(*N*-methylpyridinium-4-yl-vinyl)benzene, **MPyVB**, should have a comparatively large two-photon absorption cross section (Table 1). In support of this expectation, a cross section of $(350 \pm 50) \times 10^{-50} \text{ cm}^4 \text{ s photon}^{-1} \text{ molecule}^{-1}$ at $\sim 750 \text{ nm}$ has been reported for **MPyVB** in DMSO.³⁴

Unfortunately, any advantage accrued to this large cross section is mitigated by the fact that, unlike **TMPyP**, **MPyVB** does not produce singlet oxygen in high yield (Table 2). In a one-photon singlet oxygen phosphorescence experiment performed in H₂O, we determined that $\phi_{\Delta}(\text{MPyVB})$ is 0.02.

As perhaps one might expect, the combination of charge donating and withdrawing groups in **MPyVB** gives rise to an absorption band at comparatively long wavelengths which, in turn, imparts an orange color to the molecule (Figure 3). Moreover, **MPyVB** is highly fluorescent, with an emission profile that extends into the near-IR. In this regard, although **MPyVB** is not a viable singlet oxygen sensitizer, it could potentially be a useful, water-soluble two-photon fluorescence probe.

In light of the **MPyVB** results, an attempt was then made to modify this bis(*N*-methylpyridyl)vinylbenzene framework such as to increase the singlet oxygen quantum yield without adversely affecting the two-photon cross section. To this end, we prepared brominated derivatives (Table 2), which presumably would have a greater yield of intersystem crossing due to the heavy atom effect. Indeed, the bromines appear to effectively promote intersystem crossing as manifested by a decrease in fluorescence from these compounds relative to that observed with **MPyVB**. Nevertheless, like **MPyVB**, these molecules unfortunately still do not produce singlet oxygen in high yield (Table 2).

(ii) **Oligo(Ethylene Glycol)-Substituted Distyryl Benzenes.** It has been ascertained that, in a given sensitizer and/or sensitizer-oxygen complex, significant charge-transfer character can adversely affect singlet oxygen yields by providing an independent pathway for the deactivation of sensitizer excited states that competes with energy transfer to O₂($X^3\Sigma_g^-$).^{54,55} In the present context, we expect that the extent of intermolecular charge-transfer character in the sensitizer-oxygen complex will reflect the extent to which intramolecular charge separation

(54) Kristiansen, M.; Scurlock, R. D.; Iu, K.-K.; Ogilby, P. R. *J. Phys. Chem.* **1991**, *95*, 5190–5197.

(55) McGarvey, D. J.; Szekeres, P. G.; Wilkinson, F. *Chem. Phys. Lett.* **1992**, *199*, 314–319.

occurs in the sensitizer. With the presumption that the divinyl benzenes discussed thus far have an appreciable component of charge-transfer character, and it is this issue that limits the singlet oxygen yields, we set out to further modify this molecular framework. For the divinyl benzenes shown in Table 2, it is likely that the positively charged nitrogen in the chromophore influences the singlet oxygen yield most. To this end, a series of distyryl benzenes were prepared in which oligomeric ethylene glycol substituents were used to facilitate dissolution in water (Table 3).

To impart sufficient solubility of the sensitizer in water, it was necessary to have four or more ether substituents attached to the distyryl framework. However, all of the molecules were also soluble in toluene, and thus, singlet oxygen quantum yield measurements could be made in both solvents. On the basis of the results obtained (Table 3), several points should be noted. First, the singlet oxygen quantum yields for these molecules are noticeably larger than those obtained from the *N*-methylpyridyl-substituted divinyl benzenes. Thus, it indeed appears that we have been able to sufficiently decrease the amount of charge-transfer character that adversely influences the singlet oxygen yield. Second, as one perhaps might expect, the extent to which this CT character is manifested appears to be greater in the more polar solvent water. Thus, in comparison to quantum yields measured in toluene, the data obtained in water are systematically smaller. This result is consistent with previous observations on the effect of polar solvents on photosensitized singlet oxygen yields.^{54,56} Finally, within the error limits of our quantum yield measurements, we see that the site of ether attachment on the terminal phenyl ring (i.e., *ortho*, *meta*, or *para*) influences the data. Thus, these oligomeric ethers not only impart water solubility but, indeed, also influence the pertinent electronic properties of the chromophore.

When recording singlet oxygen data from these oligo(ethylene glycol)-substituted compounds, we also observed phenomena previously seen in other photosensitized singlet oxygen experiments.^{54,57} Specifically, as the incident laser energy was increased, the time-resolved singlet oxygen phosphorescence signal correspondingly showed an increased deviation from first-order single exponential decay kinetics. Moreover, and again as observed previously in other systems,⁵⁴ this laser energy dependent deviation from first-order behavior was significantly more pronounced in the more polar solvent. In the past, this phenomenon has been interpreted to reflect the photoinduced production of a transient species that can quench singlet oxygen and whose lifetime is somewhat shorter than that of singlet oxygen. This putative quencher is likely formed in competition with the production of singlet oxygen as a consequence of the interaction between the triplet state sensitizer and oxygen⁵⁷ and may have charge-transfer character thus explaining the observed solvent effect.⁵⁴ In support of this interpretation we found that, when using these oligo(ethylene glycol)-substituted compounds in oxygenated water, we could observe a transient luminescence signal at 1200 nm that had a lifetime of $\sim 1 \mu\text{s}$ (note that singlet oxygen does not emit at 1200 nm²⁹).

Our calculations indicate that two-photon transitions in these ether-substituted sensitizers should have cross sections larger

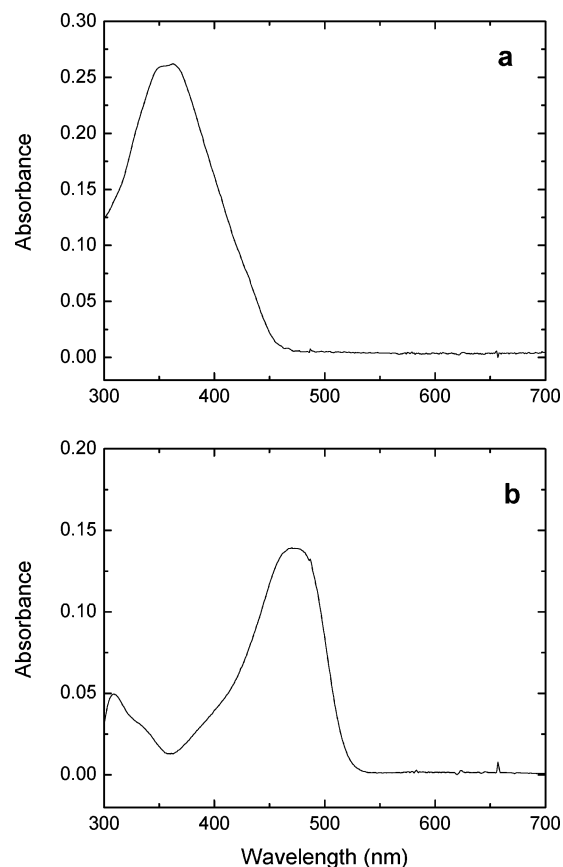


Figure 5. (a) One-photon absorption spectrum of the *ortho*, *para*-oligo(ethylene glycol)-substituted distyryl benzene in water. (b) One-photon absorption spectrum of CNPhVB in toluene.

than those in **TMPyP** but similar to those in **CNPhVB** (Table 1). However, upon examination of the corresponding one-photon absorption spectra of these molecules (Figures 3 and 5), one would expect the two-photon transitions in the ether-substituted sensitizer to be blue-shifted relative to those in **TMPyP** and **CNPhVB** (with respect to the calculated transition energies shown in Table 1, recall our caveat regarding numbers obtained at the uncorrelated Hartree–Fock level). Indeed, upon irradiation of the *ortho,para*-substituted ether over the limited wavelength range accessible with our laser system (765–845 nm) and upon comparing the relative intensities of the singlet oxygen thus produced to that produced upon irradiation of **TMPyP**, we ascertained that, in this particular spectral region, the two-photon absorption cross section for this ether was significantly smaller than that of **TMPyP**.

(iii) Porphyrazines. On the basis of our computations, we set out to examine Porphyrazine I under conditions appropriate for two-photon excitation. Although this particular porphyrazine does not have a large singlet oxygen yield ($\phi_{\Delta} = 0.13$ in toluene),⁵⁸ and although it is not sufficiently soluble in water, any information gained on this system was deemed useful.

Our computations indicate that the two lowest-energy transitions in Porphyrazine I should have the largest two-photon absorption cross sections (Table 1). Upon comparison with the spectrum shown in Figure 3, these transitions will likely be coincident with the one-photon bands at 800 and 650 nm,

(56) Abdel-Shafi, A. A.; Wilkinson, F. *Phys. Chem. Chem. Phys.* **2002**, *4*, 248–254.

(57) Gorman, A. A.; Rodgers, M. A. J. *J. Am. Chem. Soc.* **1986**, *108*, 5074–5078.

(58) Lee, S.; Stackow, R.; Foote, C. S.; Barrett, A. G. M.; Hoffman, B. M. *Photochem. Photobiol.* **2003**, *77*, 18–21.

respectively, and would thus yield two-photon bands at ~1600 and 1300 nm. Unfortunately, with our present laser system, we are unable to irradiate at these wavelengths. Over the wavelength range to which we have ready access with our existing system, Porphyrazine I has one-photon transitions that still dominate light absorption (Figure 3). Indeed, upon irradiation of a toluene solution of Porphyrazine I at 845 nm, the intensity of the singlet oxygen signal observed scaled linearly rather than quadratically with the laser intensity.

D. Sensitizer Summary. On the basis of our computational and experimental results, we draw the following general conclusions.

For the porphyrins studied, it appears that changing a substituent on a phenyl group placed at the meso position of the macrocycle does not significantly influence the magnitude of the two-photon absorption cross section. This observation may reflect a number of different phenomena, including the fact that, when in the meso position, the aromatic substituent is not an integral part of the chromophore. This latter statement is consistent with the one-photon absorption spectra of the respective molecules and with the porphyrin-sensitized singlet oxygen data. Specifically, it has been ascertained that, in a given sensitizer and/or sensitizer-oxygen complex, charge-transfer character can adversely affect singlet oxygen yields by providing a competitive pathway for the deactivation of sensitizer excited states.^{54,55} In this regard, it is important to note that the singlet oxygen yield in **TMPyP** is comparatively large ($\phi_{\Delta} = 0.77$). Thus, we infer that the positively charged *N*-methylpyridyl group in **TMPyP** does not impart a great deal of charge-transfer character to the porphyrin pi framework and, in turn, appears to be a substituent whose greatest effect is simply to impart water solubility.

In contrast, for the divinyl benzenes studied, the terminal *N*-methylpyridyl groups as well as the ether-substituted phenyl groups appear to be an integral part of the chromophore. With the *N*-methylpyridyl compound **MPyVB**, this is clearly manifested in a comparatively large two-photon absorption cross section and in a red-shifted absorption spectrum, both of which suggest electronic states with appreciable charge-transfer char-

acter. Moreover, as expected for a molecule with extensive charge-transfer character, **MPyVB** does not produce an appreciable amount of singlet oxygen.

Thus, in developing viable, water-soluble two-photon singlet oxygen sensitizers, incorporation of charge-transfer-based features that give rise to large two-photon cross sections as well as water solubility can be counterproductive; molecules with an appreciable amount of charge-transfer character are generally poor singlet oxygen sensitizers.

Conclusions

We have demonstrated that singlet molecular oxygen ($a^1\Delta_g$) can be produced and optically detected in time-resolved experiments upon two-photon excitation of a photosensitizer dissolved in water. We have outlined a number of features critical for the development of viable, water-soluble, two-photon singlet oxygen sensitizers. Molecules with functional groups that facilitate water solubility and that facilitate two-photon absorption generally have chromophores that exhibit a reasonable amount of charge transfer, and as such, these molecules unfortunately do not make singlet oxygen in high yield. Thus, in the development of an efficient water soluble two-photon singlet oxygen sensitizer, one must strike a balance between these competing influences.

Acknowledgment. This work was funded by the Danish Natural Science Research Council through a block grant for *The Center for Oxygen Microscopy*, the Danish Technical Research Council, the Danish Center for Scientific Computing, and the Villum Kann Rasmussen Foundation. The authors thank Brian M. Hoffman and Sangwang Lee (Northwestern University) for providing samples of the porphyrazines.

Supporting Information Available: Procedures for characterizing the temporal and spatial profile of the laser beam and for recording phosphorescence intensities in different solvents. This material is available free of charge via the Internet at <http://pubs.acs.org>.

JA0452020